AB

C.E. SACLAY
DSM

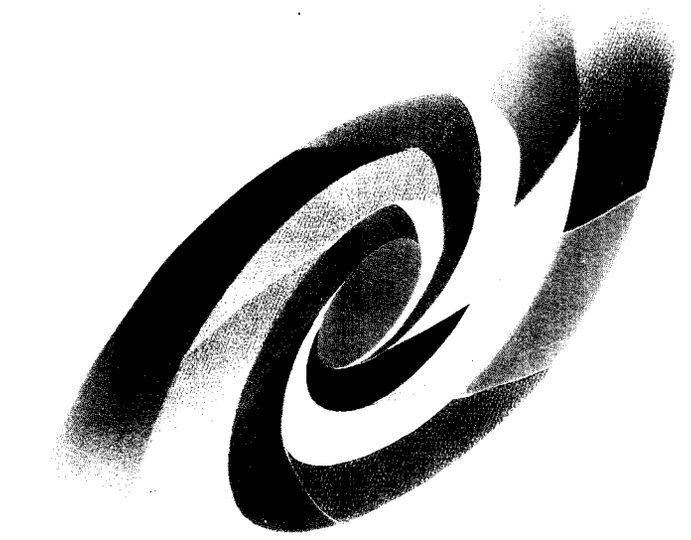

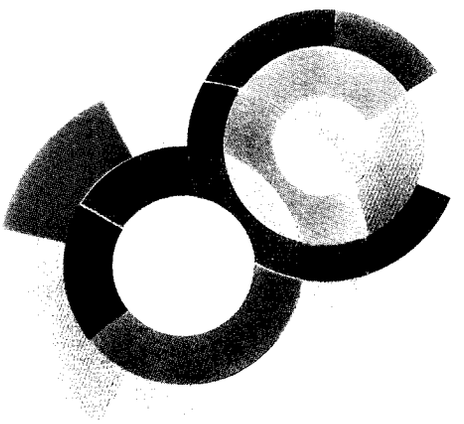

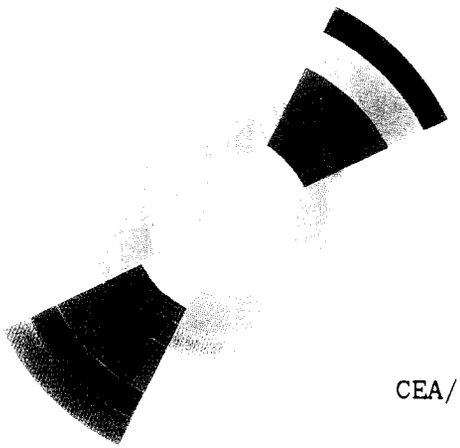

CEA/DAPNIA/SPhN 94 44 08/1994

TOTAL CROSS SECTION MEASUREMENT FOR THE THREE DOUBLE PION PRODUCTION CHANNELS ON THE PROTON

A. Braghieri, L.Y. Murphy, G. Audit,
J.M. Laget, J. Ahrens, N. d'Hose, V. Isbert,
S. Kerhoas,M. Mac Cormick, P. Pedroni,
T. Pinelli, G. Tamas, A. Zabrodin

DAPNIA

Le DAPNIA (**D**épartement d'**A**strophysique, de physique des **P**articules, de physique **N**ucléaire et de l'**I**nstrumentation **A**ssociée) regroupe les activités du Service d'Astrophysique (SAp), du Département de Physique des Particules Elémentaires (DPhPE) et du Département de Physique Nucléaire (DPhN).

Adresse : DAPNIA, Bâtiment 141
CEA Saclay
F - 91191 Gif-sur-Yvette Cedex

Soumis pour publication à :

Physics Letters B

Total Cross Section Measurement For The Three Double Pion Production Channels On The Proton

A. Braghieri[a,b], L.Y. Murphy[b,c,1], G. Audit[b], J.M. Laget[b], J. Ahrens[e], N. d'Hose[b], V. Isbert[b], S. Kerhoas[b], M. Mac Cormick[b], P. Pedroni[a], T. Pinelli[a,d], G. Tamas[b], A. Zabrodin[b,f]

[a] *INFN-Sezione di Pavia, via Bassi 6, 27100 Pavia, Italy*

[b] *CEA DAPNIA-SPhN, C.E. Saclay, 91191 Gif sur Yvette, France*

[c] *Physics Department Rensselaer Polytechnic Institute, Troy NY 12180*

[d] *Dipartimento di Fisica Nucleare e Teorica, Università degli Studi di Pavia, via Bassi 6, 27100 Pavia, Italy*

[e] *Institut für Kernphysik, Universität Mainz, 55099 Mainz, Germany*

[f] *INR, Russian Academy of Sciences, Moscow*

Abstract

Total cross-sections for the reaction channels $\gamma p \rightarrow p\pi^0\pi^0$ and $\gamma p \rightarrow n\pi^+\pi^0$, for photon energies ranging from 450 to 800 MeV, are presented here for the first time. The cross-section for the reaction $\gamma p \rightarrow p\pi^+\pi^-$ has also been obtained. These measurements were performed with the large acceptance hadronic detector DAPHNE, at the tagged photon beam facility of MAMI in Mainz.

[1] *In partial fulfillment of the requirements for the Degree of PhD in Physics*

1. Introduction

Of the three possible double pion photoproduction channels on hydrogen, only one, $\gamma p \rightarrow p\pi^+\pi^-$, has to date been measured with any accuracy [1]-[2]. Earlier experiments were for the most part performed with untagged bremsstrahlung photons incident on bubble chambers. In these instances, the $p\pi^+\pi^-$ channel was identified by the detection of at least two charged particles in coincidence. The two other possible reaction channels, each involving two neutral particles in the final state, were thus unmeasurable using such techniques.

Today, however, the availability of high intensity tagged photon beams produced at high duty factor (100%) accelerators, in conjunction with the use of large acceptance multiparticle detectors allow the direct study of these previously 'unmeasurable' channels.

In this paper, we present measurements of $\sigma_{tot}(p\pi^+\pi^-)$, $\sigma_{tot}(n\pi^+\pi^0)$, and $\sigma_{tot}(p\pi^0\pi^0)$, from threshold up to 800 MeV. In this energy range, the cross-sections should be sensitive to at least three resonances $P_{11}(1440)$, $D_{13}(1550)$, and $S_{11}(1535)$. Our results are compared with some existing models.

2. Experimental Set-Up

The experiment was performed with the large acceptance detector DAPHNE [6] installed on the tagged photon beam line [3] operated by Glasgow University, at the continuous wave accelerator MAMI in Mainz University [4]-[5].

2.1. The Photon Beam

The photon energy ranged from 350 up to 800 MeV with an average resolution of 2 MeV. The total tagged photon flux was $5{\cdot}10^6\gamma$/sec. The flux was continuously monitored throughout the experiment, such that the accuracy

of the photon normalization has been evaluated to better than $\pm 1\%$.

2.2. The Daphne Detector

We used the detector Daphne as described in ref. [6]. Some of its principal characteristics are: i) high precision measurements of the angles of emission of the charged particles, ii) good p/π particle discrimination, iii) good proton momentum resolution ($\Delta p/p$=2.5 - 10 % for p=300 - 900 MeV/c), iv) modest π^0 detection efficiency ($\leq$ 20 %), v) large solid angle acceptance (polar acceptance: $22.5° \leq \theta \leq 158.5°$ and full azimuthal acceptance $0° \leq \phi \leq 360°$), and vi) a large momentum acceptance (proton detection threshold: p_p= 280 MeV/c, and charged pion detection threshold: p_π= 78 MeV/c).

Three weaknesses are, unfortunately, inherent to the system. These are: i) no π^+/π^- discrimination, ii) no direct momentum measurement for those charged pions which do not stop in the detector, and iii) no direct measurement of the neutral pions angular distributions.

3. Data Analysis

There are five active channels in our energy range:

(a) $\gamma + p \rightarrow p + \pi^0$

(b) $\gamma + p \rightarrow n + \pi^+$

(c) $\gamma + p \rightarrow n + \pi^+ + \pi^0$

(d) $\gamma + p \rightarrow p + \pi^+ + \pi^-$

(e) $\gamma + p \rightarrow p + \pi^0 + \pi^0$

Given the characteristics of our detector, the primary identification of each channel is done in the following manner:

- Channel (d) is separated from the others by selecting events which contain two or three charged particles in coincidence.

- Channels (a), (c) and (e) are separated from the others by imposing a coincidence between a charged particle and a π^0

- Channels (a) and (e) are separated from (c) by p/π discrimination.

- Channels (a) and (e) are distinguished by the analysis of the missing mass distribution: $\gamma + p \rightarrow p + X$.

Only channel (b) cannot be uniquely identified, as the detection of a single charged π is not a sufficient condition to distinguish it from either (c) or (d). In the majority of events, this π escapes from the detector so that its momentum cannot be directly measured. Kinematical constraints, consequently, may not be applied.

3.1. The channels $\gamma p \rightarrow p\pi^0\pi^0$, $\gamma p \rightarrow n\pi^+\pi^0$, and $\gamma p \rightarrow p\pi^0$

These channels, each with at least one π^0 in the final state, are unambiguously signed by a triple coincidence between a charged particle and the two γ's resulting from the decay of the π^0. The π^0 detection efficiency as a function of photon energy, ϵ_{π^0}, was evaluated using the GEANT code. All three reactions channels were simulated with the complete set of geometrical and electronic thresholds taken into account. When relevant, neutron detection efficiencies were also included, as neutrons are sometimes capable of simulating the signature associated with γ's. This effect increases the π^0 detection efficiency by a factor of 1.15. To achieve these results, we have used the $p\pi^0$ angular distribution found in ref. [8], and have assumed a three-body phase space distribution for channels $p\pi^0\pi^0$ and $n\pi^+\pi^0$. The results from these calculations yield a global efficiency of $\epsilon_{\pi^0}(E_\gamma)$ (around) 20% for channels (a) and (c), and $\epsilon_{\pi^0}(E_\gamma)$ (around) 38% for (e).

In the second stage of the analysis, $n\pi^+\pi^0$ events are selected by p/π discrimination as in ref. [7]. Of the remaining events, distinction between $p\pi^0$ and $p\pi^0\pi^0$ events is based on the analysis of the missing mass spectrum $\gamma p \rightarrow p$ X. The good proton energy resolution is allowing us here to distinguish between final states containing one and two π^0.

As an example, we show, in fig. 1a, the missing mass spectrum at E_γ = 747 MeV. The sharp peak, corresponding to the squared mass of the π^0, is due to the two body reaction (a). We also display, on this figure, the curve resulting from a simulation, which takes into account the various experimental resolutions as well as the known angular distribution associated with reaction (a). On the other hand, the low bump found at higher squared masses, corresponds clearly to the three body process (e). It has also been fitted with a three-body phase space angular distribution . The contributions from processes (a) and (e) are clearly separated.

Protons from the reaction $\gamma p \rightarrow p\eta$ can also be detected for $E_\gamma \geq 780$ MeV, and for $\theta_p \leq 24.5°$. The missing mass distribution, subject to these constraints, is shown on fig. 1b where we see a well defined peak associated with η production. These η's are principally detected via their neutral mode of decay and show up initially in the $p\pi^0$ coincidence spectrum. This contamination is easily eliminated by applying a cut at M_X^2=0.28 GeV^2. It contributes of the order of 1 μb at 785 MeV, as shown in figure 3b.

Fig. 2 shows our results for the reaction channel $\gamma p \rightarrow p\pi^0$ compared with data from ref. [8], integrated over our detector's acceptance. The excellent agreement between these results inspires confidence in our ϵ_{π^0} values as well as in our p/π discrimination.

3.2. The Channel $\gamma p \rightarrow p\pi^+\pi^-$

The measurement of this channel was the most straightforward. The only sizable contamination possible comes from the channels with a π^0, when

either the π^0 disintegrates into γe^+e^- or a photon from the π^0 converts into a e^+e^- pair prior to entering the wire chambers. In such cases, the leptons can be mistaken for charged π's, giving rise to a 2 or 3 charged particles events. A simulation of these processes, using GEANT, predicts a contamination level of 4% of the total $p\pi^0$ counting rate. This is in agreement with the measured counting rate of 2-particles events at 350 MeV. Knowing the $p\pi^0$, $p\pi^0\pi^0$ and $n\pi^+\pi^0$ cross sections this contamination is easily subtracted. We infer that the additional contamination to the $\gamma p \rightarrow p\pi^+\pi^-$ cross section from $p\eta$ photoproduction is of the order of 2 μb at 800 MeV.

Finally, as the kinematics of events where three charged particles were detected in coincidence are overdetermined, we have found that on the order of 1% of such events were rejected by kinematical constraints. We surmise from this that the contamination due to 3 pions events is at most on the order of 1%, which, in the present energy domain, is negligible.

4. Results

Fig. 3a-b-c show the results for the three double pion photo-production channels, with the corresponding numerical values listed in tables 1, and 2. The measured cross-section integrated over the acceptance of the detector are represented by filled circles. Assuming a 3-body phase-space distribution, we have extrapolated this data to obtain the total cross-section, as shown by the open circles. Based on this assumption, we found that, at 700 MeV, we are accessing no less than 80% of the $n\pi^+\pi^0$ cross-section, but only about 50% of $p\pi^0\pi^0$. We also feel that this supposition is the principal source of systematic error.

We note that, in complete agreement with previously published data, but with markedly improved precision, $\sigma_{tot}(p\pi^+\pi^-)$ exhibits a rapid rise from 450 to 600 MeV, and then saturates. This is in contrast to $\sigma_{tot}(n\pi^+\pi^0)$ and $\sigma_{tot}(p\pi^0\pi^0)$ which continue to rise smoothly to about 720 MeV.

In fig 4 we show the ensemble of partial channels. The cross sections taken for processes $\gamma p \rightarrow n\pi^+$ and $\gamma p \rightarrow p\pi^0$ are the integrated values of the differential cross sections of ref. [8]. The sum of the 5 channels is in good agreement with the total hadronic cross section on the proton obtained by Armstrong et al.[9] except at high energy where the contribution of the $\gamma p \rightarrow p\eta$ channel has to be taken into account.

Finally, we compare, in fig. 5a-b-c, our experimental results with the models calculated by Oset [11] and two of us (J.M.L and L.Y.M).

The data for the photoproduction of two charged pions are well reproduced by the model of Lüke et al [13], which takes into account the production of a $\pi\Delta$ intermediate state. This state is either directly excited, as modeled by two diagrams (contact and pion exchange) of the Born term [10], or produced by the decay of N^* resonances, namely the $D_{13}(1520)$ and $P_{11}(1440)$, as described in ref. [12]. Unitarity is empirically taken into account by introducing an absortive factor, related to $\pi\Delta$ scattering, into the basic expression as prescribed by Lüke and Söding in ref. [13].

We have improved on this model by adding all possible 2π decay channels of the resonances, $\pi\Delta$ as well as correlated pion pairs. We have parametrized the 2π states as σ or ρ mesons. Furthermore every parameter of our model is taken from the recent works of Arndt [14]-[15]-[16]-[17] and Manley [18], and so are by no means free. For the D_{13}, both the electric and magnetic excitation mechanisms were taken into account, as well as its subsequent decay into the $\pi\Delta$ channel in both the S and D-waves.

Figure 5a shows the various contributions to the reaction $\gamma p \rightarrow p\pi^+\pi^-$ which are: 1) the Born term, 2) the combined contributions of the above and the D_{13}, showing clearly the interference of the electric part of the D_{13} with the Born term, and 3) the small contribution of the P_{11}, which itself does not interfere with the Born term.

For the $p\pi^0\pi^0$ channel, the Born term is suppressed since the photon

does not couple with neutral pions. This allows the direct measurement of the resonances. It appears clearly that an important contribution to the cross-section of the $p\pi^0\pi^0$ channel stems from the P_{11} resonance decaying into an '$N\sigma$' state (fig. 5b). In this case we have set the decay width of the σ to be 50 MeV, which is consistent with the upper limit published [19], but higher than Manley's, which is 33±10 MeV.

Finally, it appears from figure 5c that our underestimating of the above reaction around 700 MeV is even more pronounced in the $n\pi^+\pi^0$ channel, where our model is a full factor 2 lower than the data. Other mechanisms, such as possibly ρ and ω exchange, may play a role. It might also be a hint that the phenomenological way in which unitarity is implemented is not adequate. A coupled channel treatment is clearly needed.

5. Conclusion

We have successfully measured the three hydrogen double-pion photoproduction channels. The form of the cross-section of the triple charged channel differs markedly from the other two and our model, which does accurately reproduce the $p\pi^+\pi^-$ channel, as well as the general trend of the $p\pi^0\pi^0$ channel, does not succeed in reproducing the behavior of the $n\pi^+\pi^0$.

References

[1] ABBHHM Collaboration, Phys. Rev. 175 (1968) 1669

[2] G. Gialalella et al., Nuovo Cimento 63A (1969) 892

[3] I. Anthony et al., Nucl. Instr. and Meth. A301 (1991) 230

[4] H. Herminghaus et al., Nucl. Instr. and Meth. A138 (1976) 1

[5] H. Herminghaus et al., Proc. 1990 Linear Accelerator Conf., Albuquerque 1990, preprint LA-12004-C

[6] G. Audit et al., Nucl. Instr. and Meth. A301 (1991) 473

[7] A. Braghieri et al., Nucl. Instr. and Meth. A343 (1994) 623

[8] Landolt-Börnstein, Photoproduction of Elementary Particles, Group 1-Vol. 8, ed. H. Schopper (Springer-Verlag, Berlin, 1973)

[9] T.A. Armstrong et al., Phys. Rev. D5 (1972) 1640

[10] J.M. Laget, Phys. Rep.. 69 (1981),1

[11] J.A. Tejedor, E. Oset, Nucl. Phys. A571 (1994) 667.

[12] D. Lüke et al., Nuovo Cimento 58A (1968) 234.

[13] D. Lüke, P. Söding, Springer Tracks in Modern Physics 59 (1971) 39.

[14] R.A. Arndt et al, Phys. Rev. C42 (1990) 1853.

[15] R.A. Arndt et al, Phys. Rev. C42 (1990) 1864.

[16] R.A. Arndt et al, Phys. Rev. D43 (1991) 2131.

[17] R.A. Arndt et al, Phys. Rev. D43 (1992) 3995.

[18] D.M. Manley et al, Phys. Rev. D45 (1992) 4002.

[19] Particle Data Group, Phys. Rev. D45 (1992).

Figure captions

1. a) Top: Missing mass distribution at E_γ = 747 MeV for protons in coincidence with a π^0. The curves are the results of simulations for the processes $\gamma p \rightarrow p\pi^0$ and $\gamma p \rightarrow p\pi^0\pi^0$. (See text for details).
   b) Bottom: Missing mass distribution for protons at forwards angles and in coincidence with a π^0. The peak at the highest masses comes from the reaction $\gamma p \rightarrow p\eta$.

2. Measured cross section for the reaction $\gamma p \rightarrow p\pi^0$. The curve was obtained by integrating over the detector acceptances the differential cross section in [8] .

3. Total cross section for the three channels: the filled circles represent the measured cross sections and the open circles the extrapoled cross sections by assuming a phase space distribution:
   a) $p\pi^+\pi^-$ compared with the previously published data.
   b) $p\pi^0\pi^0$: extrapolations are of the order of 50%. The contribution from $\gamma p \rightarrow p\eta$ is also shown.
   c) $n\pi^+\pi^0$.

4. The different contributions of the three double–pion photoproduction channels measured in the present experiment and compared with the total cross section on the proton [9]. The open circles also include the two single–pion channels [8]. No errors were taken for the laters.

5. Comparison of the data with the models.
   a) $p\pi^+\pi^-$: Our complete model is shown by the solid curve, along with the contributions from the Born term (dashed line), and the combination of the Born and the full D_{13} terms (dotted line). For comparison, Oset's model is described by the dot-dashed curve.
   b) $p\pi^0\pi^0$: Our complete model is shown by the solid line, along with

the contributions from the D_{13} (dashed line), the P_{11} decaying into the $\pi\Delta$ channel (dotted line) and into the $N\sigma$ channel (dot-dashed line). c) $n\pi^+\pi^0$: Once again, the complete model is described by the solid curve, along with the contributions from the Born term (dashed line), and the full D_{13} term (dotted line).

TABLE 1

Total cross section for $\gamma p \rightarrow p\pi^+\pi^-$

E_γ (MeV)	$\sigma(p\pi^+\pi^-)$ (μb)	E_γ (MeV)	$\sigma(p\pi^+\pi^-)$ (μb)	E_γ (MeV)	$\sigma(p\pi^+\pi^-)$ (μb)
419 ± 6	4.0 ± 0.3	431 ± 6	4.5 ± 0.3	443 ± 6	6.2 ± 0.3
454 ± 5	7.1 ± 0.3	464 ± 5	9.0 ± 0.3	474 ± 5	12.0 ± 0.4
485 ± 6	15.3 ± 0.4	497 ± 6	20.9 ± 0.5	509 ± 6	26.2 ± 0.6
521 ± 6	30.8 ± 0.6	533 ± 6	36.0 ± 0.7	545 ± 6	41.7 ± 0.7
556 ± 5	47.0 ± 0.8	566 ± 5	53.1 ± 0.8	576 ± 5	57.7 ± 0.9
586 ± 5	61.1 ± 0.9	596 ± 5	61.8 ± 1.0	606 ± 5	67.2 ± 1.0
616 ± 5	69.2 ± 1.0	626 ± 5	70.8 ± 1.0	636 ± 5	72.7 ± 1.1
645 ± 4	74.7 ± 1.1	653 ± 4	74.9 ± 1.2	661 ± 4	75.7 ± 1.1
670 ± 5	75.9 ± 1.1	680 ± 5	76.7 ± 1.2	690 ± 5	75.4 ± 1.2
699 ± 4	75.8 ± 1.2	707 ± 4	76.0 ± 1.2	715 ± 4	75.6 ± 1.2
723 ± 4	75.4 ± 1.2	731 ± 4	74.2 ± 1.2	739 ± 4	75.0 ± 1.2
747 ± 4	73.6 ± 1.2	755 ± 4	71.7 ± 1.2	763 ± 4	70.7 ± 1.1
771 ± 4	69.9 ± 1.2	779 ± 4	68.0 ± 1.2	787 ± 4	71.9 ± 1.6

TABLE 2

Total cross section for $\gamma p \rightarrow n\pi^+\pi^0$ and $\gamma p \rightarrow p\pi^0\pi^0$

E_γ (MeV)	$\sigma(n\pi^+\pi^0)$ (μb)	$\sigma(p\pi^0\pi^0)$ (μb)
464 ± 15	2.2 ± 0.1	3.3 ± 0.3
497 ± 18	5.0 ± 0.2	5.5 ± 0.4
533 ± 18	11.0 ± 0.3	6.8 ± 0.4
566 ± 15	17.9 ± 0.5	8.6 ± 0.4
596 ± 15	23.5 ± 0.6	8.0 ± 0.4
626 ± 15	27.7 ± 0.7	9.6 ± 0.5
653 ± 12	34.6 ± 0.8	10.5 ± 0.5
680 ± 15	44.1 ± 0.9	11.1 ± 0.5
707 ± 12	51.4 ± 1.0	12.1 ± 0.5
731 ± 12	54.9 ± 1.1	11.7 ± 0.6
755 ± 12	56.3 ± 1.1	10.3 ± 0.5
779 ± 12	49.0 ± 1.1	10.1 ± 0.6

FIG. 1

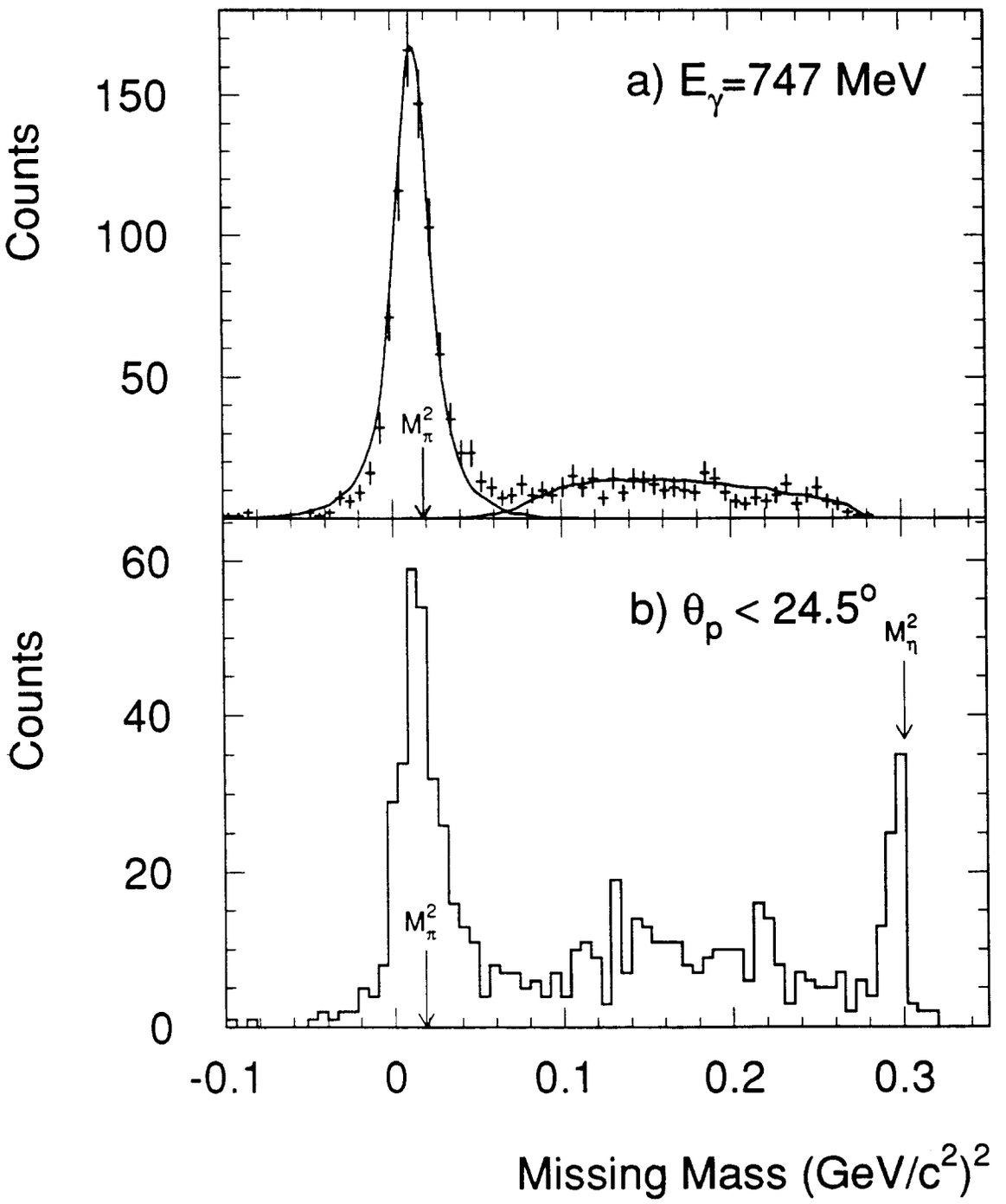
a) E_γ=747 MeV
Counts
150
100
50
M_π^2
b) $\theta_p < 24.5^o$
M_η^2
M_π^2
Counts
60
40
20
0
-0.1
0
0.1
0.2
0.3
Missing Mass $(GeV/c^2)^2$

FIG. 2

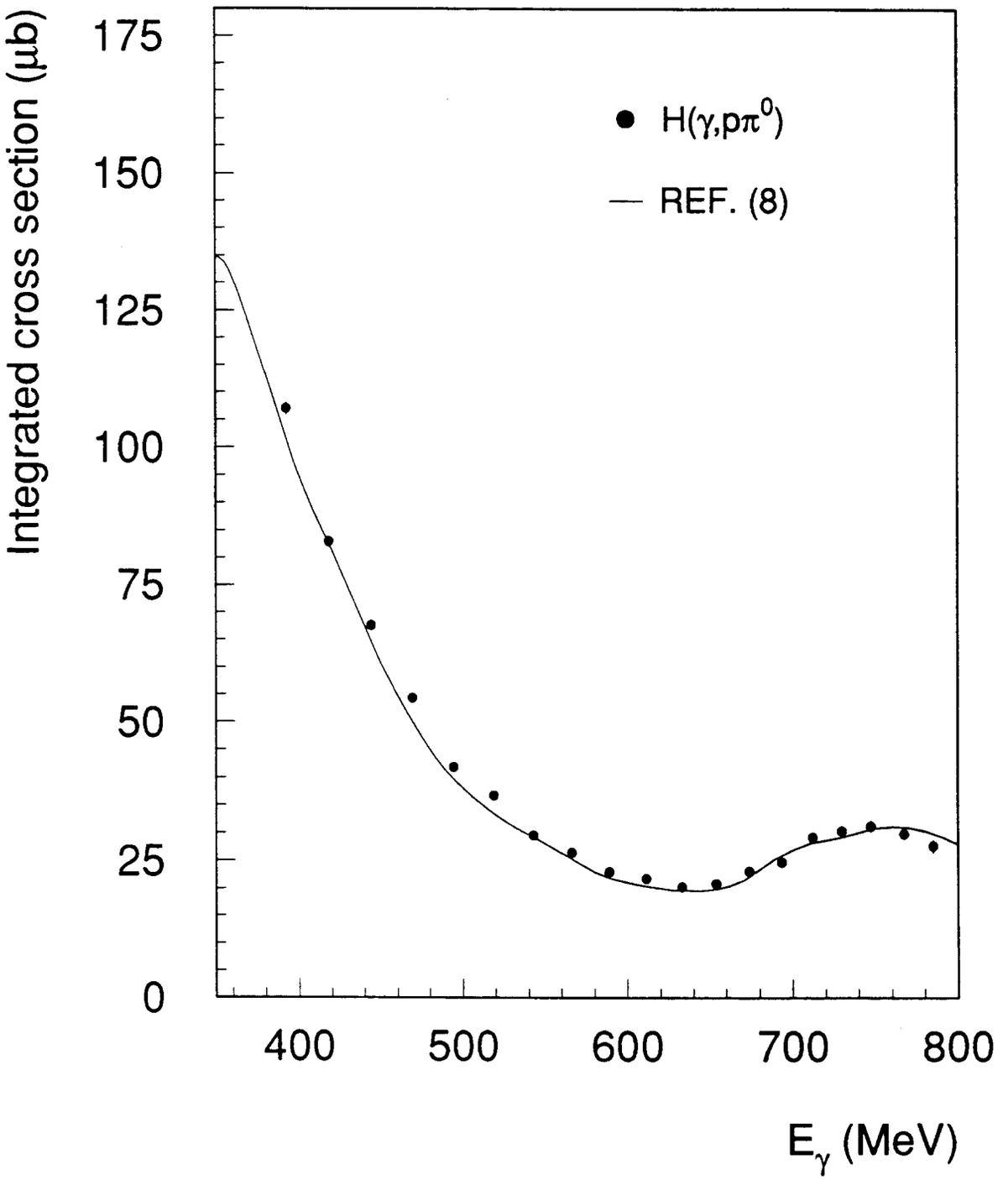
Integrated cross section (μb)
175
150
125
100
75
50
25
0
400
500
600
700
800
E_γ (MeV)
$H(\gamma,p\pi^0)$
REF. (8)

FIG. 3

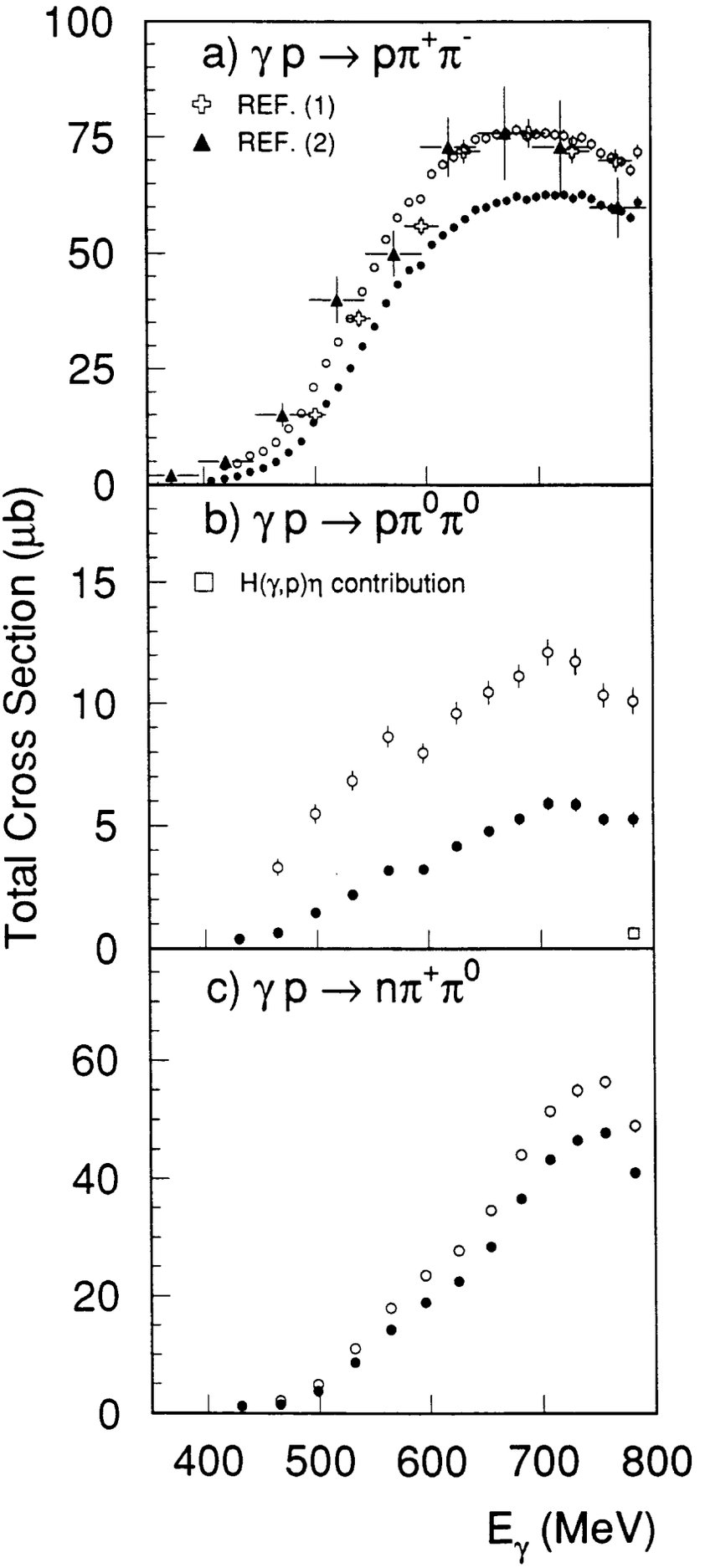
a) γ p → pπ+π-
REF. (1)
REF. (2)
b) γ p → pπ0π0
H(γ,p)η contribution
c) γ p → nπ+π0
Total Cross Section (μb)
100
75
50
25
0
15
10
5
0
60
40
20
0
400
500
600
700
800
Eγ (MeV)

FIG. 4

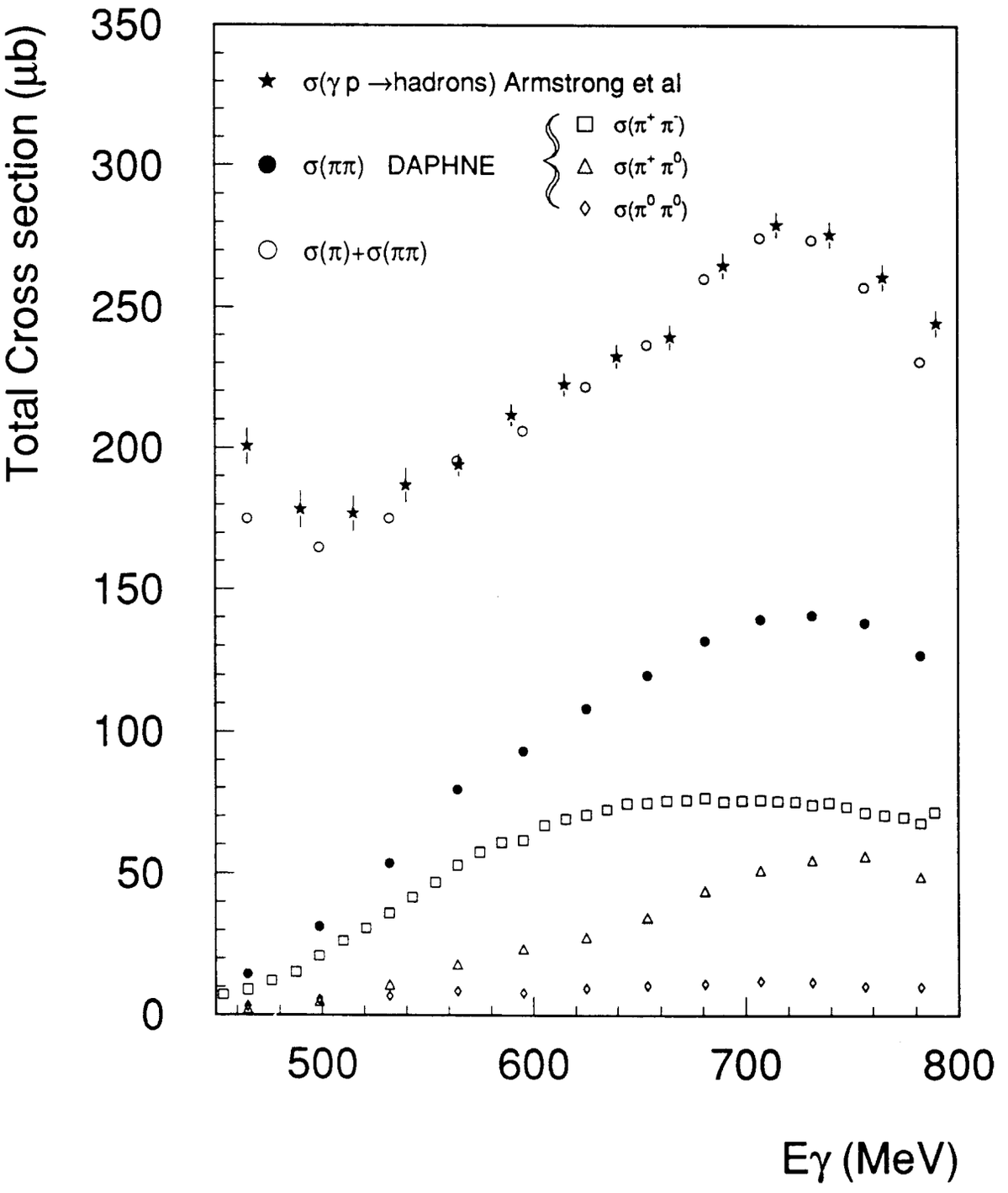
Total Cross section (μb)
350
300
250
200
150
100
50
0
500
600
700
800
Eγ (MeV)
σ(γ p →hadrons) Armstrong et al
σ(ππ) DAPHNE
σ(π)+σ(ππ)
σ(π⁺ π⁻)
σ(π⁺ π⁰)
σ(π⁰ π⁰)

FIG. 5

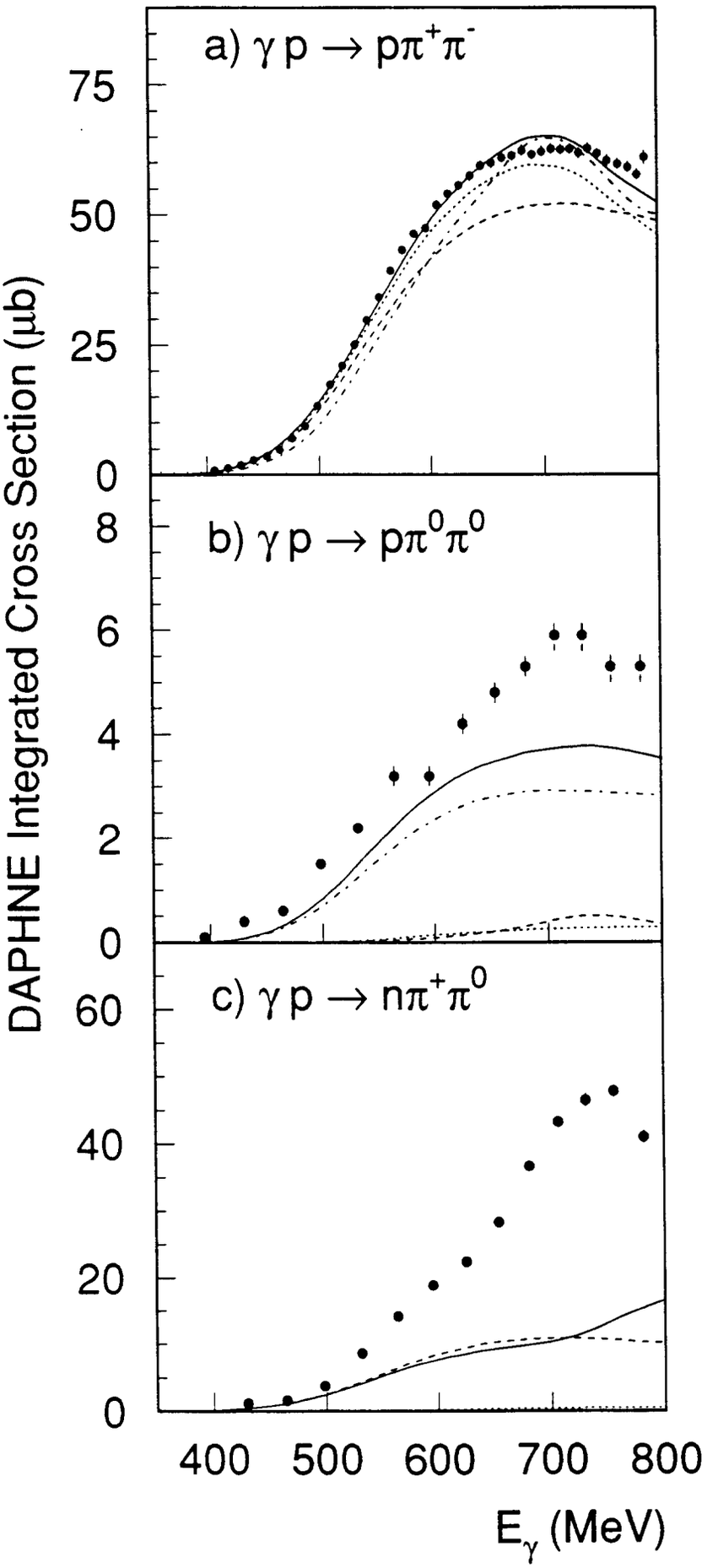
a) γ p → pπ+π-
b) γ p → pπ0π0
c) γ p → nπ+π0
DAPHNE Integrated Cross Section (μb)
75
50
25
0
8
6
4
2
0
60
40
20
0
400
500
600
700
800
Eγ (MeV)